# Troubleshooting of Von Karman Induced Penstock Protection Valve Resonance at FMHL+

**C Nicolet[1], S Alligné[1], M Furrer[2], D Fischer[2], J Grognuz[3], O Chène[4] and B Valluy[4]**

[1] Power Vision Engineering Sàrl, CH-1024 Ecublens, Switzerland
[2] HYDRO Exploitation SA, CH-1951 Sion, Switzerland
[3] CADFEM (Suisse) AG, CH-1020 Renens, Switzerland
[4] ALPIQ SA, CH-1001 Lausanne, Switzerland

christophe.nicolet@powervision-eng.ch

**Abstract**. The FMHL power plant was originally a 240 MW pumped-storage power plant in Switzerland, put in operation in 1971 which installed capacity was extended to 480 MW in 2016 with maximal output power set to 420 MW including 60 MW as reserve. The significant increase of the total discharge of the power plant in generating mode from 32 $m^3/s$ at 240 MW to 57 $m^3/s$ at 420 MW might be critical due to the higher flow velocity throughout the different safety valves of the power plant. During commissioning, the discharge was increased stepwise from 32 to 57 $m^3/s$ while monitoring the vibration of the safety valves. Significant vibration amplitudes have been recorded at a frequency of 62.5 Hz on the penstock protection valve for a discharge of 43 $m^3/s$. Von Karman vortex shedding induced resonance on the stiffener of the bi-plan valve obturator was then suspected. The paper presents troubleshooting of this resonance problem, where CFD and FEM investigations have been performed to define appropriate trailing edge modifications of the obturator stiffener plates able to significantly reduce the Von Karman dynamic lift coefficient and thus reduce drastically vibration amplitudes.

## 1. Introduction

The FMHL power plant was originally a 240 MW pumped-storage power plant in Canton Vaud Switzerland, put in operation in 1971. In 2016 the installed capacity was extended to 480 MW with maximal output power set to 420 MW including 60 MW as reserve, see Figure 1. FMHL, Forces Motrices Hongrin-Léman SA belongs to the shareholders Romande Energie SA, Alpiq Suisse SA, Groupe E SA and City of Lausanne. Alpiq, as owner’s representative, was in charge of the extension project FMHL+ and the operator is Hydro Exploitation SA.

To accommodate the significant increase of the total discharge of the power plant in generating mode from 32 $m^3/s$ at 240 MW to 57 $m^3/s$ at 420 MW, it was necessary to build a new surge tank in order to achieve safe transient behavior for both generating and pumping modes, [1]. Another aspect which might be critical in case of increase of power plant capacity, is the higher flow velocity throughout the different safety valves of the power plant. Therefore, during the commissioning of the two new ternary units of 120 MW each in 2016, see Figure 2, the vibration of both the penstock protection valve and the upper reservoir intake valves were monitored. During the discharge stepwise increase from 32 to 57 $m^3/s$ significant noise and vibration amplitudes have been recorded at a frequency of 62.5 Hz on the penstock protection valve for a discharge of 43 $m^3/s$. Von Karman vortex shedding induced resonance on the stiffener of the bi-plan valve obturator was then suspected, see [2], [3]. The paper presents troubleshooting of this resonance problem, which was based on numerical investigation using both CFD analysis of the flow through the butterfly valve and FEM of the valve mechanical structure. The simulation results enabled to point out possible resonances in good agreement with the site measurements. To prevent the hydro-mechanical resonance problem, it is possible either i) to avoid a match between mechanical natural frequency and excitation source frequency, ii) to reduce excitation source amplitudes or iii) to increase the system damping, [4]. In the case of the FMHL+ penstock protection valve, modifications of the stiffener plates' trailing edge were investigated with CFD. A significant reduction of the Von Karman dynamic lift coefficient was achieved, which drastically reduced the vibration amplitudes.

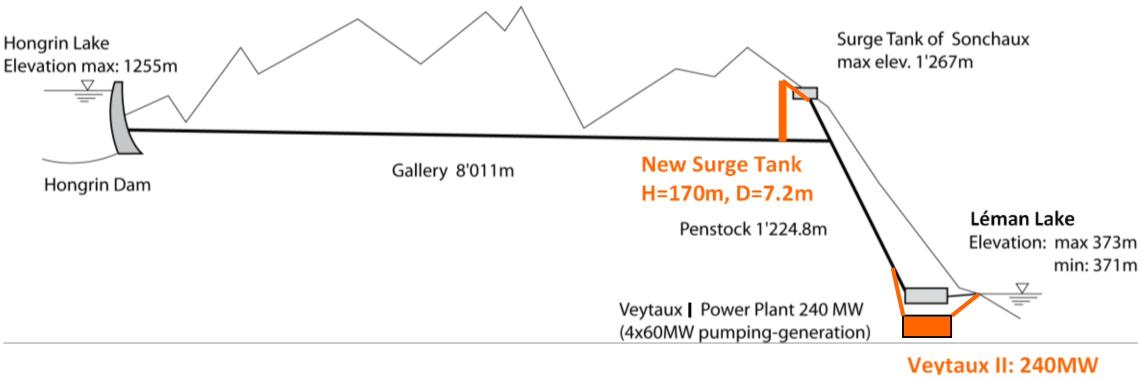


**Figure 1.** Layout of the FMHL power plant with existing Veytaux I powerhouse with 240 MW total capacity and the Veytaux II powerhouse with additional 240 MW.

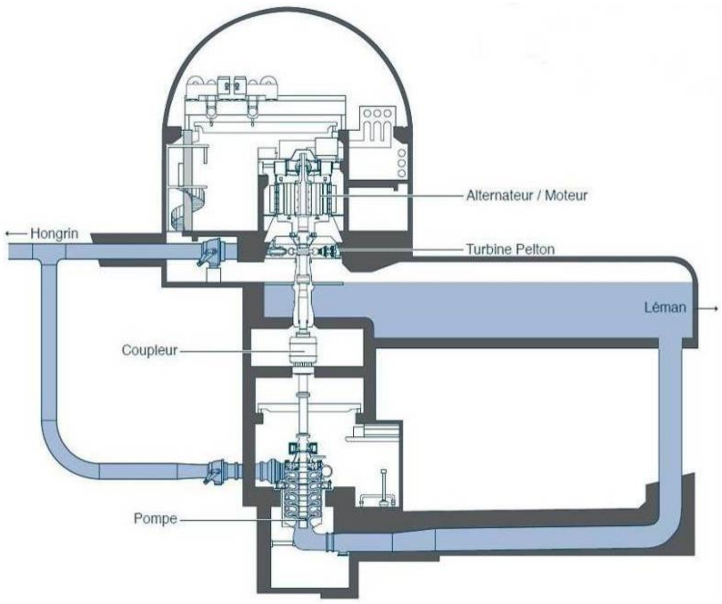


**Figure 2.** Cross-sectional view of the ternary Unit of Veytaux II Powerhouse.

## 2. Identification of the resonance problem

The first observation of high noise and vibration level at the 2.9 m diameter bi-plan butterfly penstock protection valve of FMHL, see Figure 3, was performed on 17.6.2016 for a discharge of 43 $m^3/s$ and characterized by a resonance frequency of 62.5 Hz. Then, detailed vibration investigation was performed on 11.7.2016 with installation of several accelerometers on the valve, its servomotor and on the upstream and downstream pipe. For the second measurement campaign, the maximum vibration amplitude at

62.5 Hz was found for a discharge of 49 $m^3/s$ when operating at 360 MW and the maximum amplitude of vibration amplitude of 11 mm/s was measured on the pipe wall downstream of the valve, see Figure *4*. The difference between the two tests was attributed to the influence of local static pressure, see [5]. Such vibration level being above acceptable limit, thorough investigation was undertaken, while operation in the range 330 MW and 380 MW was forbidden. The measurement of the pipe wall vibration was also installed for long term monitoring and an alarm was included in the SCADA system to detect any excessive pipe wall vibration.

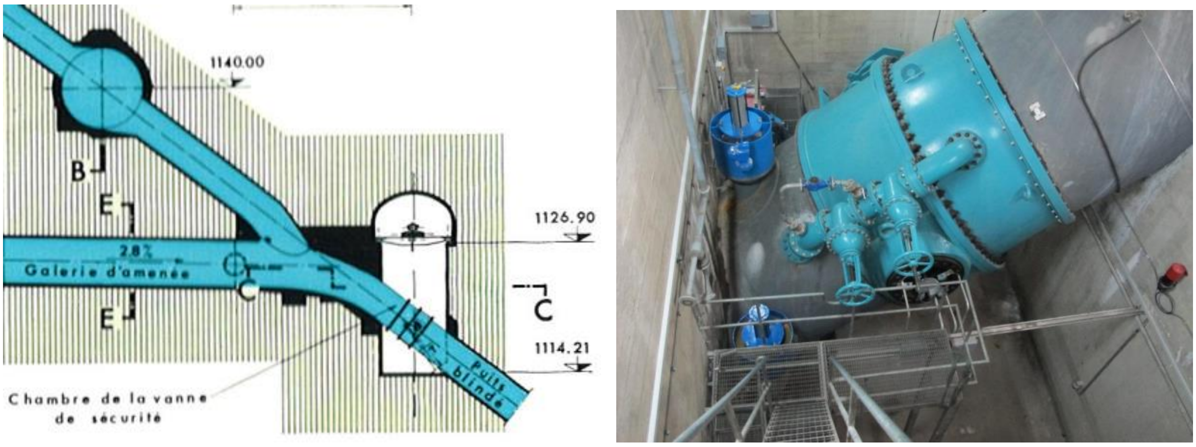


**Figure 3.** Penstock protection valve ($D_{ref}$=2.9 m) cross-sectional view (left) and site configuration (right).

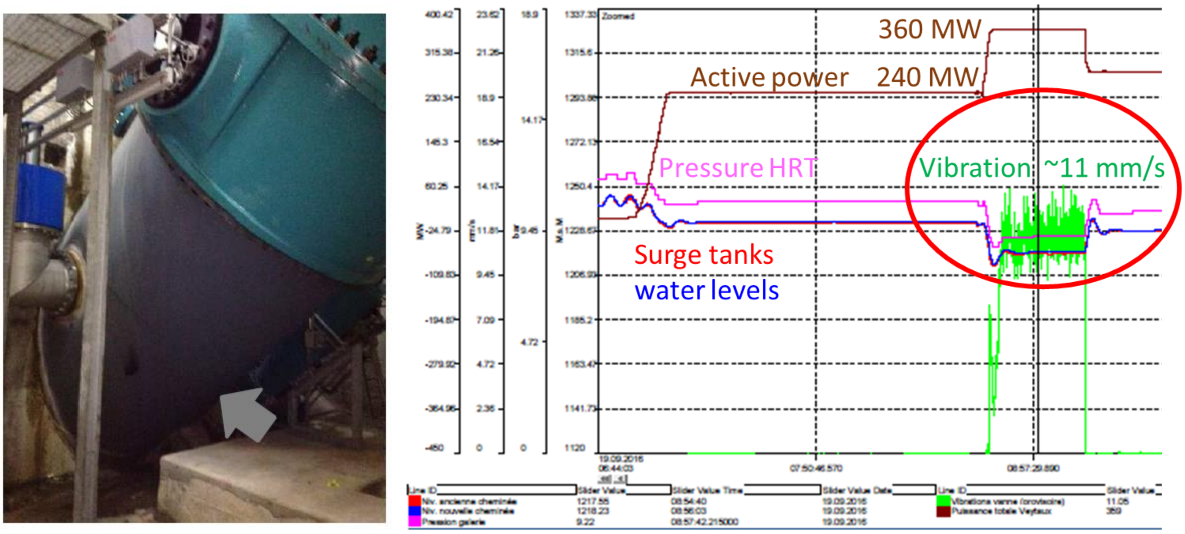


**Figure 4.** High vibration level measured on the pipe wall downstream the penstock protection valve.

First, the frequency of Von Karman vortex shedding can be estimated with Strouhal number expected to be in the range from 0.2 to 0.24 for the trailing edge of a hydrofoil, see Table 1, leading to the following condition:

$$Str = \frac{f \cdot \delta_w}{C_{ref}} = \sim 0.2 - 0.24 \qquad (1)$$

Where:

- f: Von Karman vortex Shedding frequency (Hz)
- $\delta_w$: Characteristic dimension, foil thickness (m)
- $C_{ref}$: Reference velocity (in free stream) (m/s)

Based on the discharge of 49 m$^3$/s, leading to a reference flow velocity through the valve obturator cross-sectional area of 7.7 m/s, and a frequency of 62.5 Hz, a hydrofoil thickness of 25 to 30 mm is estimated. Therefore, a hydromechanical resonance between Von Karman vortex shedding and the structure of one of the obturator stiffener "AA" or "BB", see Figure 13, having a steel plate thickness of 35 mm could be suspected. As the trailing edge of these stiffeners already featured asymmetric chamfers with an angle of 15° and some truncation, a CFD analysis was performed to confirm Von Karman vortex frequency and determine the corresponding dynamic lift coefficient given by:

$$\zeta = \frac{2 \cdot F}{\rho \cdot {C_{ref}}^2 \cdot \delta_w \cdot B} \qquad (2)$$

Where:

- F: Amplitude of dynamic lift force (N)
- B: Foil width (m)
- ρ: Fluid density (kg/m$^3$)

However, at this stage of the investigation, the link between possible hydromechanical resonance between Von Karman vortex shedding from the stiffener AA and the downstream pipe wall was not obvious. It was not clear if the energy was convected by the fluid or was transferred through the mechanical structure. In parallel, a Finite Element Method, FEM, analysis of the penstock protection valve structure was conducted in order to check the plausibility of hydromechanical resonance at a frequency of 62.5 Hz.

**Table 1.** Strouhal numbers and pressure fluctuations amplitudes relative to blunt trailing edge (RA) for different trailing edge shape [6].

| Trailing edge | Geometry | | | | RA |
|---|---|---|---|---|---|
| Blunt | $\delta_w$ | | | | 1 |
| Semi-circle | $\delta_w$ | | | | 2.6 |
| Symmetrically sharpened | $\delta_w$ $\alpha$ | $\alpha$ | 30° | | ≈ 0 |
| | | | 45° | 0.2 | 0.45 |
| | | | 60° | | 4 |
| | | | 90° | to | 3 |
| Sharpened on one side | $\delta_w$ $\alpha$ | $\alpha$ | <10° | | > 2 |
| | | | 30° | 0.24 | 0.1 |
| | | | 45° | | 0.4 |
| | | | 60° | | 0.5 |
| Sharpened on one side and rounded | $\delta_w$ $\alpha$ | $\alpha$ | 30° | | < 0.2 |
| | | | 45° | | < 0.5 |
| Hollow | $\delta_w$ | | | | < 0.5 |

## 3. CFD analysis

First a 3D steady state CFD computation of flow structure through the valve was conducted using the ANSYS-CFX 16.2 simulation software taking into account the influence of the upstream bend, see Figure 3, with a 1.7 million nodes unstructured finite volume mesh extending 10 times the valve diameter upstream the valve (corresponding approximately to cutting plane E-E in Figure 3) and 5 times the valve diameter downstream the valve. The simulation results presented in Figure 5 shows that despite some minor asymmetry of the velocity profile upstream the valve obturator, a 2D flow assumption around the stiffener plates AA and BB is rather fair, and also show some recirculation zone characterized with high vorticity, behind the obturator trunnion.

Then, a refined 2D unsteady CFD computation with high spatial resolution in the hydrofoil boundary layer was undertaken to capture Von Karman vortices around stiffener plates AA and BB, see geometry in Figure 6. The simulation performed with a structured mesh enabled to demonstrate that Von Karman vortex shedding was developing at the trailing edge of the stiffener plate AA which is characterized by a simulated frequency of 68.3 Hz, corresponding to an error of about 9% as compared to the measured frequency, and a dynamic lift coefficient of $\zeta=0.31$ was deduced, see corresponding unsteady pressure field in Figure 7.

However, the simulation performed at the trailing edge of stiffener plate BB did not show Von Karman vortex shedding and thus the dynamic lift coefficient corresponds to $\zeta=0$, see corresponding unsteady pressure field in Figure 8. The main reason of the difference between the flow that develop at the trailing edge of the stiffeners AA and BB is probably linked to the aspect ratio $s/\delta_w$, where s is the chamfer length, which is larger for the stiffener plate BB $s/\delta_w = 2.67$ than for the stiffener plate AA for which $s/\delta_w = 2.13$, even though they are both above the values $s/\delta_w = 1.5$ which is often considered as the limit above which the dynamic lift forces vanish, see [4], [7].

Based on these CFD results, it was concluded that only the stiffener AA shall be subject to hydromechanical resonance, as the excitation amplitude related to the stiffener BB was extremely low. In addition the stiffener AA should have a lower structure eigenfrequency than the stiffener BB due to the different plate width, see Figure 13, and thus shall be the first structure subject to resonance when the flow was increased. In addition, CFD simulations have also been performed for symmetrical 30° chamfer with a radius of 2 mm, see Figure 9, supposed to lead to a dynamic lift coefficient equal to zero, see Table 1, which was confirmed by CFD.

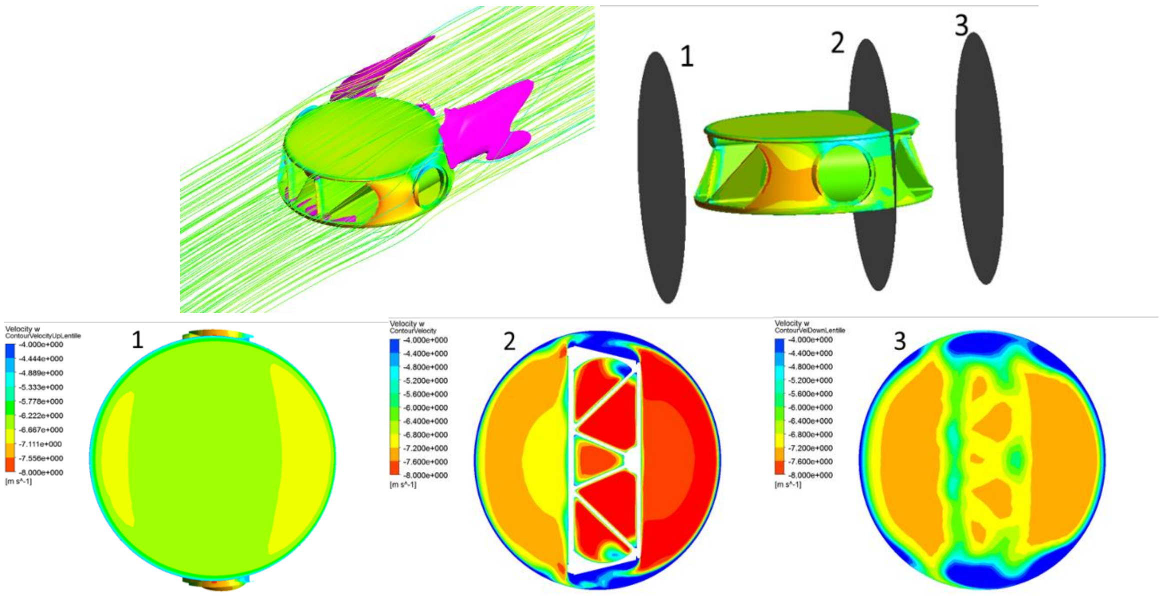


**Figure 5.** 3D steady state flow and corresponding stream lines and vorticity (violet) (top left), pressure field and sections numbering (top right) and velocity contour plots at sections 1, 2 and 3 (bottom).

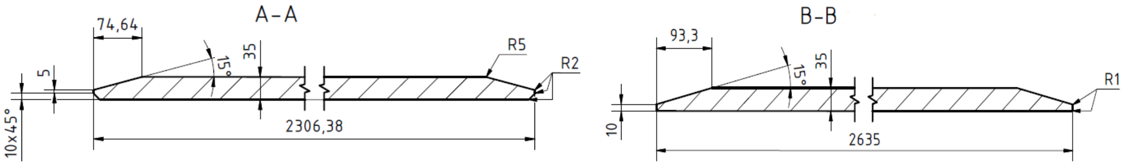


**Figure 6.** Geometry of stiffener AA (left) and BB (right).

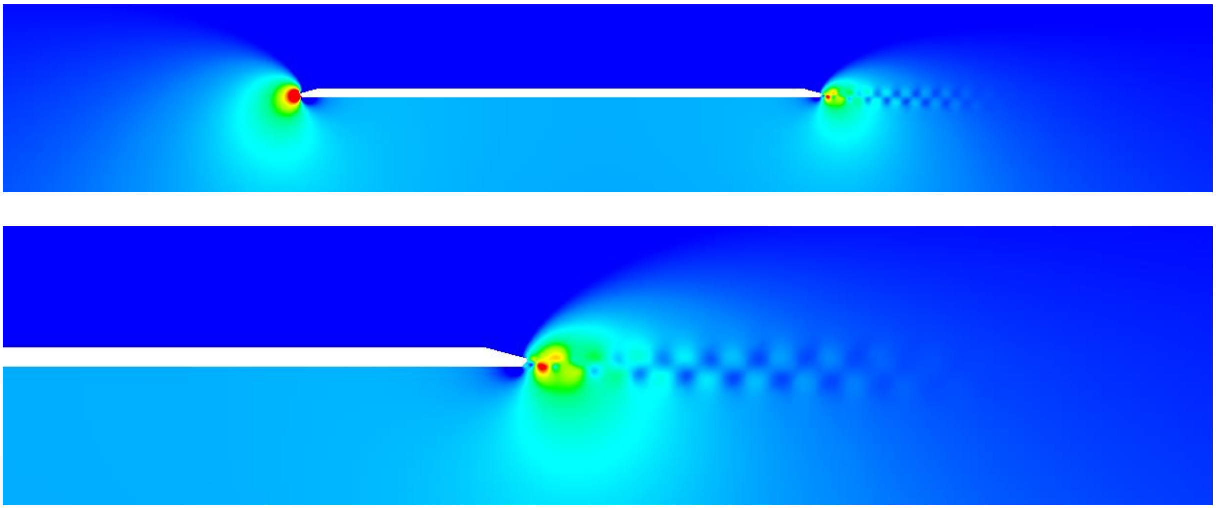

**Figure 7.** Unsteady pressure field obtained with 2D CFD of the flow around the stiffener “AA”, full domain (top) and zoom at trailing edge (bottom).

**Figure 8.** Unsteady pressure field obtained with 2D CFD of the flow around the stiffener “BB”.

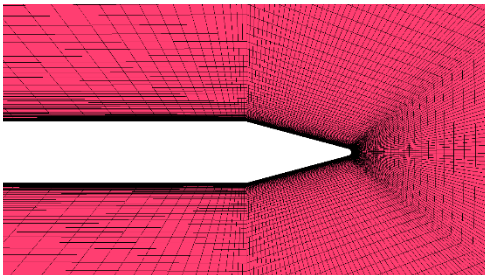

**Figure 9.** 2D mesh of the modified profile symmetrical 30° with radius 2 mm for unsteady CFD simulation.

## 4. FEM analysis

The Figure 10 presents the mesh of the 3D FEM non-linear model of the penstock protection valve of FMHL which includes the valve body, the valve obturator, the servomotor and counter weight, the by-pass valve, the upstream and downstream pipes with the connection to the concrete civil structure and the water modelled with acoustic elements. The contact with friction between the mechanical component is considered, while no-movements boundary conditions are applied at the concrete wall structure to represent the concrete wall embedding effect. A constant height dependent hydrostatic internal pipe pressure corresponding to 130 mWC is applied on the internal walls. The computation of the structure eigenfrequencies performed with the ANSYS software revealed several natural frequencies in the range 0 to 100 Hz. One of the most relevant eigenmode of the penstock protection valve found at 67.2 Hz is presented in Figure 11.

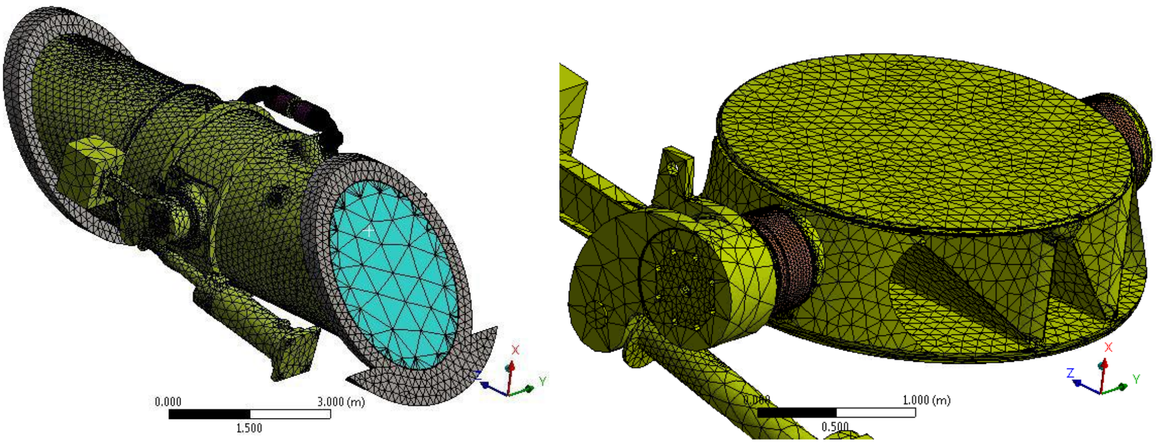


**Figure 10.** Mesh of the FEM including water acoustic element (left) and details of the obturator mesh (right).

It is interesting to note that this mode shape, which features 7.5% difference on the frequency observed during the site measurements, involves significant deformation of both the bending mode of the stiffener plate AA and of the diametrical mode of the pipe downstream of the valve, as described by Kito [5]. The fact that this natural frequency of the stiffener plate and the one of the downstream pipe are very close to each other might explain some coupling between hydromechanical resonance taking place between the stiffener AA and its Von Karman vortex shedding and the downstream pipe wall. In addition, the location of the pipe with high deformation matches well the location of highest amplitudes measured at site, see Figure 4.

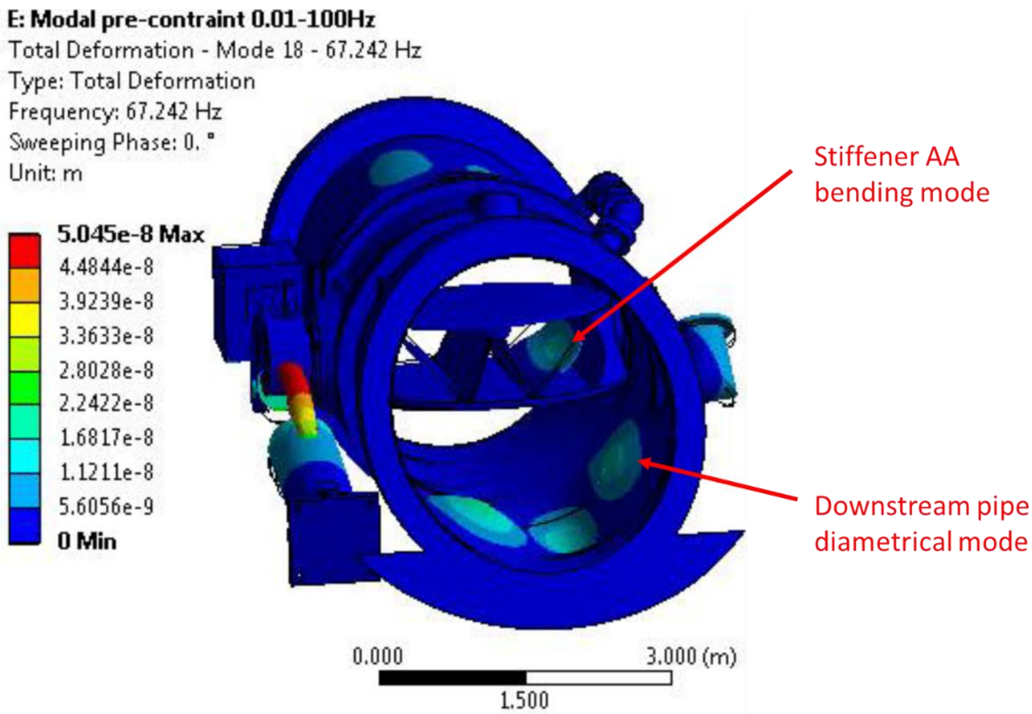


**Figure 11.** Eigen mode of the structure with combined stiffener AA bending mode with downstream pipe wall diametral mode computed for an eigenfrequency of 67.2 Hz.

## 5. Temporary and final solution implementation

In order to confirm the excitation mechanism between Von Karman vortex shedding at the stiffener AA trailing edge and the downstream pipe wall vibration pointed out from CFD and FEM analysis, a simple site test was conducted on 3.11.2016 and which results are reported in Figure 12. A first reference test was performed to confirm the presence of the hydromechanical resonance phenomena. A second test was performed with and without a wedge on pipe wall but is not commented in this paper. Then a third test was performed with an incidence angle imposed to the obturator in order to disturb the boundary layer that develops along the stiffener plate AA, which indeed suppressed the Von Karman vortex shedding and thus also drastically reduced the noise and the pipe wall vibration from 8 mm/s down to below 2 mm/s. This third test confirmed the excitation mechanism between the stiffener AA Von Karman vortex shedding and the pipe wall vibration.

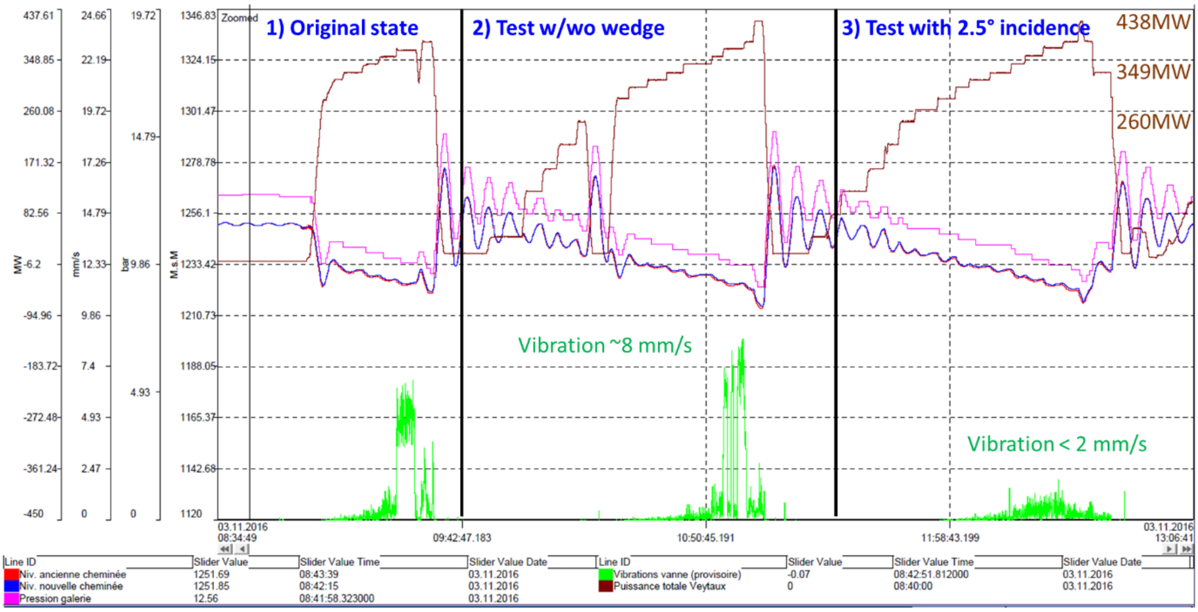


**Figure 12.** Vibration measured on the pipe wall downstream the penstock protection valve for normal conditions (left) with and without application of a wedge (center) and with obturator incidence angle of 2.5° (right).

It was then decided to modify the stiffener AA according to the proposed geometry with 30° symmetrical chamfer, see Figure 9, which aims at reducing excitation from the Von Karman induced dynamic lift coefficient down to zero. However, the modification of the stiffeners AA trailing edge has to be performed on site in difficult condition due to the important inclination of the penstock protection valve of about 79% (angle of 38°). This site work requires a long interruption of the power plant production necessary to dewater the headrace tunnel and part of the penstock and to install temporary scaffolding structure, and then perform the modification of the trailing edges by grinding.

A temporary solution was undertaken, and consists in applying artificial sand roughness (~40 grit) at the trailing edge of the stiffener plates AA, as indicated in Figure 13 and Figure 14 left, again to disturb the boundary layer at the trailing edge of the stiffener plate, and affect the shedding of the Von Karman vortices. This temporary solution was applied at site on stiffener plates AA within a very limited production interruption without need to install any specific structure. The tests performed after application of the artificial roughness end of November 2016 showed that this solution shifted the discharge for which resonance may occur, and significantly reduced the vibration level at the penstock protection valve and enabled to extend the operating range of the power plant. This solution also confirmed that the resonance was due to the Von Karman induced resonance on stiffener AA.

Finally, after 8 months operation with the temporary solution, in August 2017, the trailing edge of the stiffener AA was modified according to the proposed geometry in Figure 9, see execution in Figure 14 right, which fully solved the vibration issue on the FMHL penstock protection valve and on the downstream pipe wall, see final results before and after trailing edge modification in Figure 15.

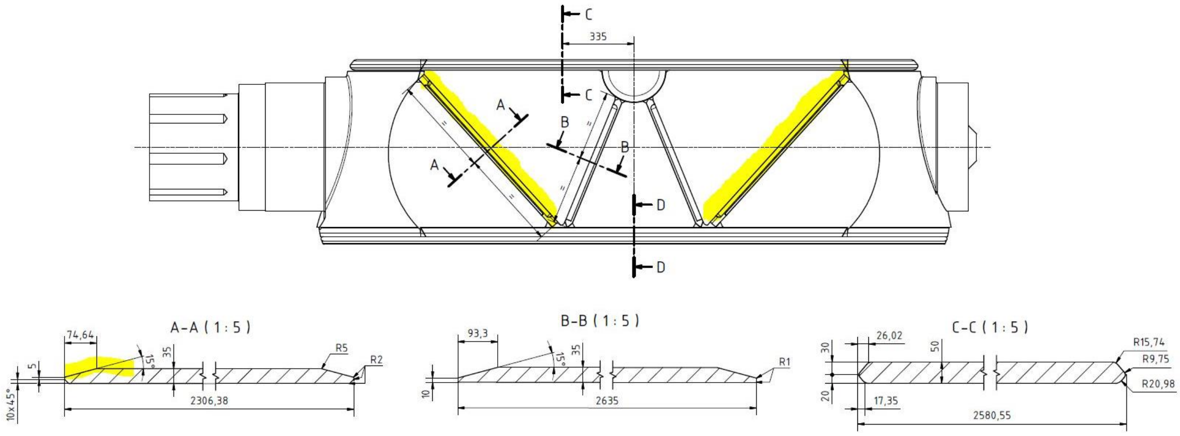


**Figure 13.** Penstock protection valve bi-plan obturator and indication of the area where artificial sand roughness was applied on stiffener AA.

**Figure 14.** Photograph of artificial sand roughness applied at the trailing edge of the stiffener plate AA as temporary solution (left) and final trailing edge profile with 30° angle after trailing edge site grinding as long-term solution (right).

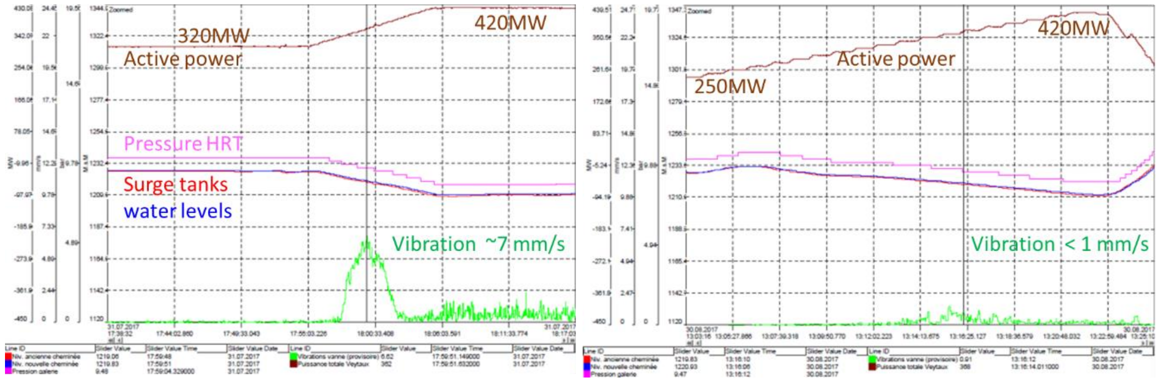


**Before** trailing edge modification 31.7.2017 **After** trailing edge modification 30.8.2017

**Figure 15.** Site measurement of pipe wall vibration downstream the penstock protection valve level during active power ramp-up before (left) and after final trailing edge profile with 30° angle modification (right).

## 6. Conclusion

The increase of nominal discharge from 32 to 57 m$^3$/s resulting from power upgrade at FMHL PSPP from 240 MW to 420 MW induced a hydromechanical resonance of the penstock protection valve between obturator stiffener and Von Karman vortex shedding inducing a peculiar high vibration level phenomena of the pipe wall downstream the valve. CFD and FEM analysis enabled to perform root cause analysis, and propose mitigation measures based on the reduction of the excitation source by modifying the stiffener trailing edge shape based on CFD simulations. A temporary solution based on artificial roughness applied at the trailing edge of the stiffener enabled safe operation over 8 months, after which a final modification was applied to fully solve the vibration problems.

**Acknowledgement**

The authors would like to acknowledge Mr. Etienne Vuadens from HYDRO Exploitation SA who performed the site measurements. The authors also would like to thank Mr. Pierre-Yves Lowys from GE Renewable for the constructive exchanges during root cause analysis.

## References

[1] Nicolet C, Béguin A, Dayer J-D, Micoulet G, 2018, Hydraulic transient challenges for the upgrade of FMHL+ pumped storage power plant from 240MW to 420MW, Proc. of the 29th IAHR Symposium on Hydraulic Machinery and Systems, Kyoto, Japan, Sept 16-21, 2018, paper 104.

[2] Plichon J-N and Lescure A, 1979, Hydraulic instability effects in power station, La Houille Blanche N°2/3-1979, pp.: 103-108.

[3] Li J, Zhong S, Wang Z, Pang L, Jia W, 2014, Analysis of cracks in butterfly valve of Francis turbine, Journal of Hohai Universty (natural Science), Vol 42, No5, Sept. 2014, pp.: 451-454.

[4] Dörfler P, Sick M and Coutu A, 2013, Flow-Induced Pulsation and vibration in Hydroelectric Machinery, Springer-Verlag London 2013.

[5] Kito F, 1959, The Vibration of penstocks, Water Power, October 1959, pp.: 379-392.

[6] Gülich J F, 2008, Centrifugal Pumps, Springer-verlag Berlin Heidelberg 2008.

[7] Neidhardt T, Jung A, Hyneck S and Gummer J, 2018, An alternative approach to the Von Karman vortex problem in modern hydraulic turbines, Hydropower & Dams, Issue 3, 2018, pp.:58-62.